Supporting Information

High-Performance Co_4S_3-MnS-MoS_2@CC Catalysts for Hydrogen Evolution Reaction

Sizhan Shu[a, 1], Denglin Zhu[a, 1], Xuejun Wang[a], Jun Sun[a], Jiani Wang[a], Qian Ling[a], Zile Zhou[a], Yujia Chen[a], Pingfan Wu[a,b *]

[a]*Hubei Univ Technol, Institute of POM-based Materials,Hubei Prov Key Lab Green Mat Light Ind, New Mat & Green Mfg Talent Intro & Innovat Demonst, Wuhan 430068, China,*

[b] *Hubei Longzhong Lab, Xiangyang 441000, Hubei, Peoples R China*

[*] Corresponding authors.

E-mail address: pingfanwu-111@163.com (P. Wu).

E-mail address: 13995976671@163.com (S. Shu).

[1] These authors contributed equally in this work.

Experiment

Testing methods:

Fourier transform infrared (FT-IR) spectra were measured on a Nicolet iS50 infrared spectrometer using KBr pellets. X-ray diffraction (XRD) patterns were tested on an X-ray diffractometer (Rigaku Ultima IV, Cu Kα radiation λ=0.154178 nm). X-ray photoelectron spectra (XPS) were tested on an ESCALAB 250Xi equipped with ex situ treatment chamber and the binding energy of C1s (284.8 eV) was used as the reference to correct the measured binding energy. Scanning electron microscopy (SEM) images were obtained on a cold-field emission BUCT. The atomic absorption test results were obtained on the German continuous light source atomic absorption spectrometer (GB/T 15337-2008). High resolution transmission electron microscopy (HRTEM) images and elemental mapping results were obtained on a Tecnai G2 F20 U-TWIN.

Electrochemical testing

All electrochemical tests were conducted at room temperature

using a CHI760E electrochemical workstation. The electrocatalytic performance of the materials was evaluated using a three-electrode system, with reference electrodes being Hg/Hg_2Cl_2 in 0.5 M H_2SO_4 and Hg/HgO in 1 M KOH, a graphite rod serving as the counter electrode, and a modified carbon cloth as the working electrode with a geometric area of 1 cm × 1 cm. The potentials for all reversible hydrogen electrode (RHE) measurements were calculated using the equations $E_{RHE} = E_{Hg/HgO} + 0.098 + 0.059$ pH for 1 M KOH and $E_{RHE} = E_{Hg/Hg2Cl2} + 0.244 + 0.059$ pH for 0.5 M H_2SO_4.

Linear sweep voltammetry (LSV) was performed in both 1 M KOH and 0.5 M H_2SO_4 electrolytes with a scan rate of 2 mV/s. Tafel plots were fitted to the linear regions of the Tafel equation ($\eta = a + b \log j$). Electrochemical impedance spectroscopy (EIS) was conducted over a frequency range of 0.01 kHz to 100 kHz with an amplitude of 5 mV and a test potential of 0.1 V. Furthermore, cyclic voltammetry tests were carried out within a potential range of 0.1 V to 0.2 V at scan rates of 10, 20, 30, 40, 50, 60, 70, and 80 mV/s. All data were corrected for a 90% IR drop.

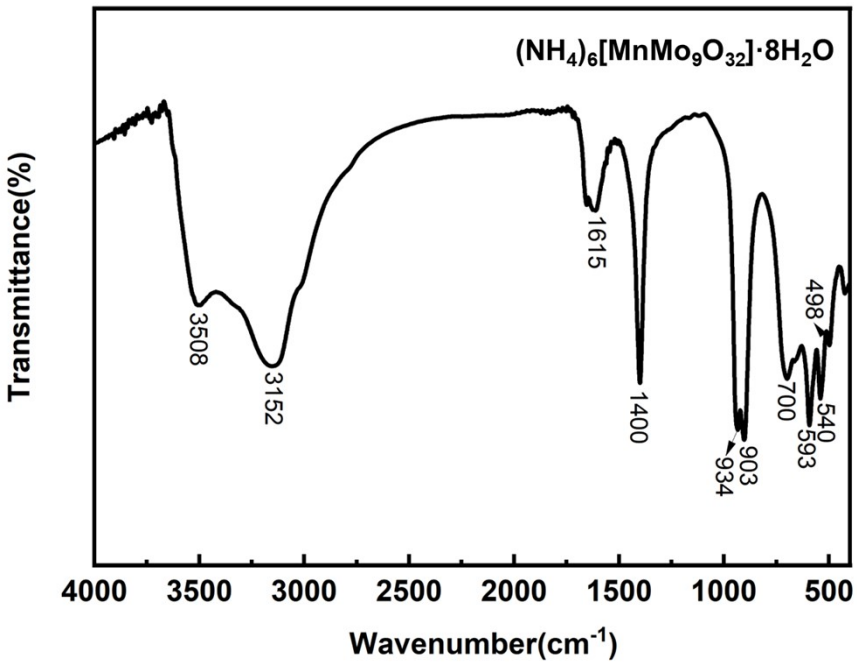

Fig. S1. Infrared spectrum of $MnMo_9$

Synthesis of $(NH_4)_6[MnMo_9O_{32}]\cdot 8H_2O$: Initially, 1 mmol of ammonium paramolybdate was dissolved in 10 mL of deionized water, and the pH was adjusted to 5.1 with glacial acetic acid. Then, 7 mmol of manganese sulfate was dissolved in 10 mL of deionized water, and the two solutions were mixed. The mixture was stirred

and heated to boiling, resulting in a yellow precipitate. Subsequently, 2 mmol of sodium persulfate was dissolved in 5 mL of water and added to the aforementioned mixture, which was then heated to a solution temperature of 80°C, turning the solution orange-red. This temperature was maintained for approximately 30 minutes, after which the solution was left to stand overnight at room temperature until orange-red crystals precipitated. The crude product was obtained after filtration, washing, and air-drying. The product was recrystallized three times to yield the crystalline product $MnMo_9$.

IR Characterization of $MnMo_9$: The synthesized polyoxometalate $MnMo_9$ was characterized by Fourier-transform infrared spectroscopy, as shown in Fig. S1. The infrared spectrum revealed characteristic absorption peaks for water molecules' O-H bonds at 3508 cm^{-1} and 1615 cm^{-1}; vibrational absorption peaks for NH^{4+} at 3152 cm^{-1} and 1400 cm^{-1}; and peaks in the range of 1000 cm^{-1} to 400 cm^{-1}, which are characteristic of Waugh-type polyoxometalate anions, with specific absorption peaks at 934 cm^{-1} and 903 cm^{-1} arising from the stretching vibrations of Mo=O; peaks at 700 cm^{-1}, 593 cm^{-1}, and 540 cm^{-1} resulting from the bending vibrations of Mo-O-Mo; and the characteristic absorption peak at 498 cm^{-1} resulting from the bending vibrations of Mn-O-Mo. All the aforementioned peaks are consistent with those described in the literature.[1]

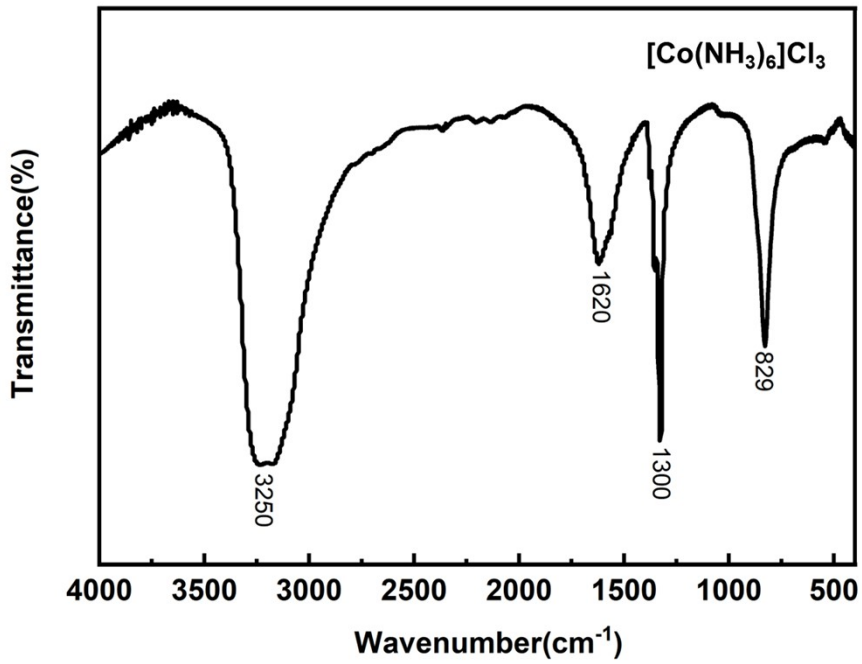

Fig. S2. Infrared spectrum of $[Co(NH_3)_6]Cl_3$

Synthesis of $[Co(NH_3)_6]Cl_3$: Initially, 110 mmol of ammonium chloride was dissolved in 12 mL of deionized water and heated to boiling. Then, 70 mmol of cobalt chloride was added to the ammonium chloride solution, which was dissolved upon heating and then transferred to a beaker containing 0.5 g of activated carbon. After cooling, 20 mL of concentrated ammonium hydroxide was added, and the mixture was cooled again to below 10°C. Under stirring, 8 mL of a 10% hydrogen peroxide solution was slowly added, and the temperature was raised to 60°C and maintained for 20 minutes, followed by cooling again. Then, 75 mL of a 0.5 mol/L hydrochloric acid aqueous solution was added, and the mixture was heated to boiling. After the precipitate dissolved, it was filtered while hot. To the filtrate, 20 mL of 6 mol/L hydrochloric acid was slowly added, resulting in the precipitation of an orange-yellow product. This product was cooled with ice water, filtered, and washed with cold dilute

hydrochloric acid, and then air-dried.

IR Characterization of $[Co(NH_3)_6]Cl_3$: Fig. S2 shows the infrared spectrum of $[Co(NH_3)_6]Cl_3$. The spectrum displays four major characteristic absorption peaks: (1) a strong absorption peak at 829 cm^{-1} corresponding to the Co-N rocking vibration, (2) a sharp absorption peak at 1300 cm^{-1} corresponding to the symmetric bending vibration of the N-H bond, (3) an absorption peak at 1620 cm^{-1} corresponding to the asymmetric bending vibration of the N-H bond, and (4) an absorption peak at 3250 cm^{-1} corresponding to the asymmetric stretching vibration of the N-H bond. These are highly consistent with those reported in the literature[2], indicating that we have successfully synthesized $[Co(NH_3)_6]Cl_3$.

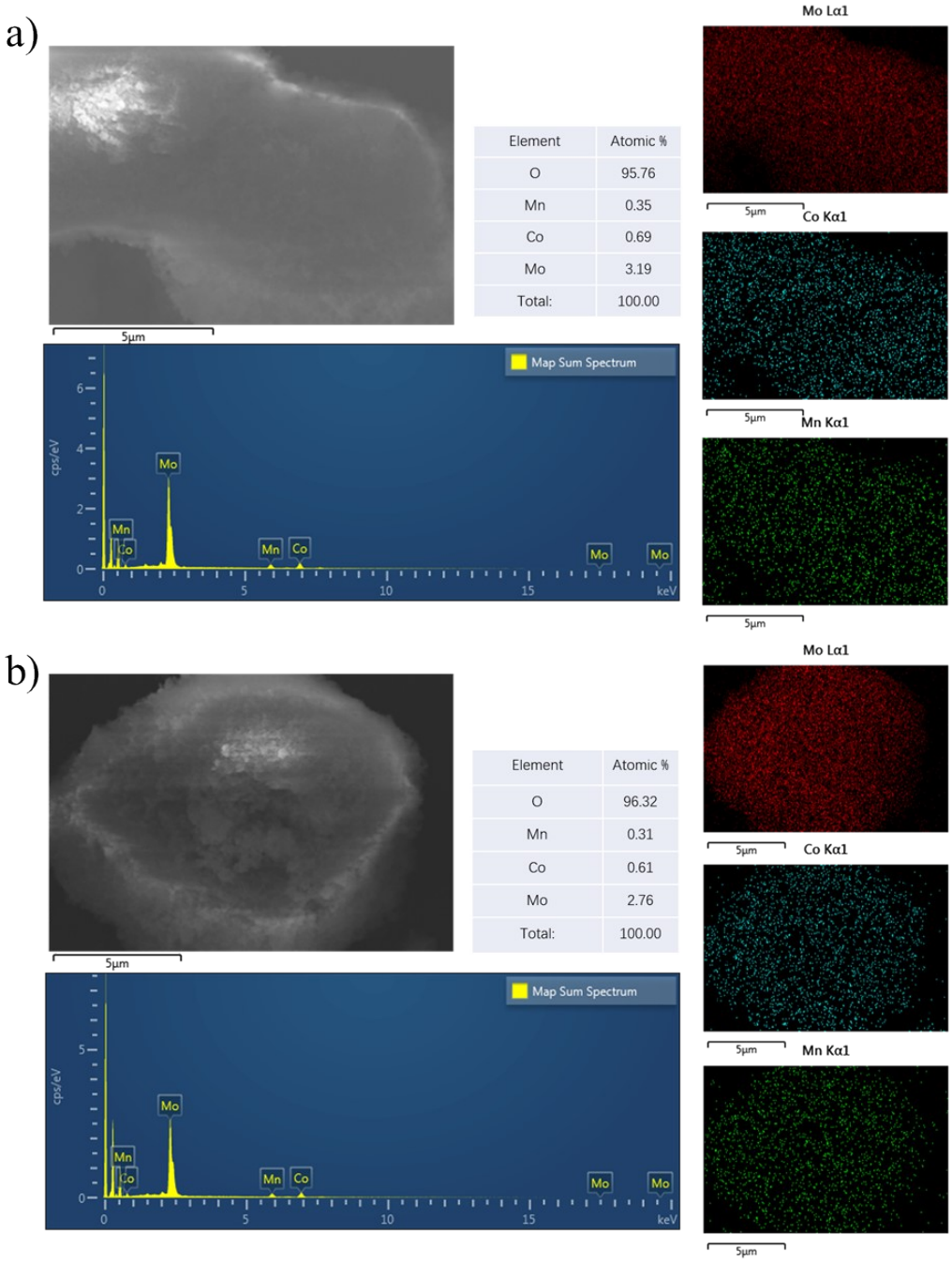

102 **Fig. S3. EDS images of the Co_2MnMo_9**

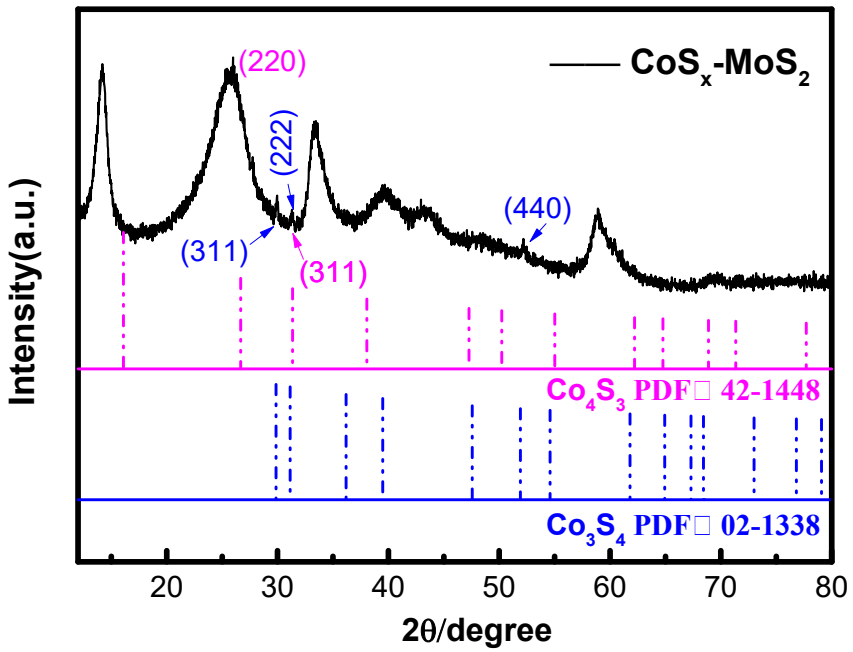

103

104 **Fig. S4. XRD patterns of the Co_xS-MoS_2@CC**

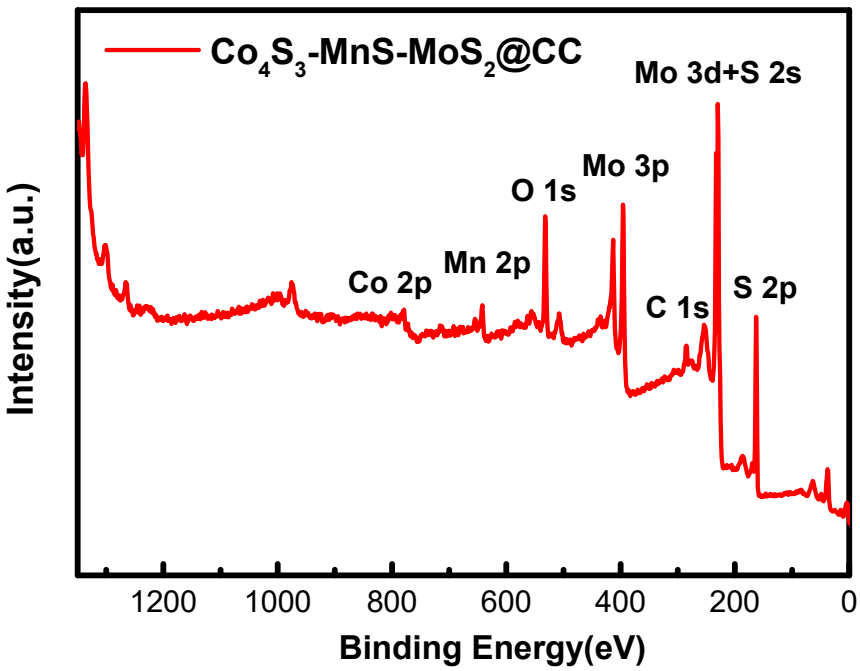

105 **Fig. S5. full survey XPS spectra of the Co_4S_3-MnS-MoS_2@CC**

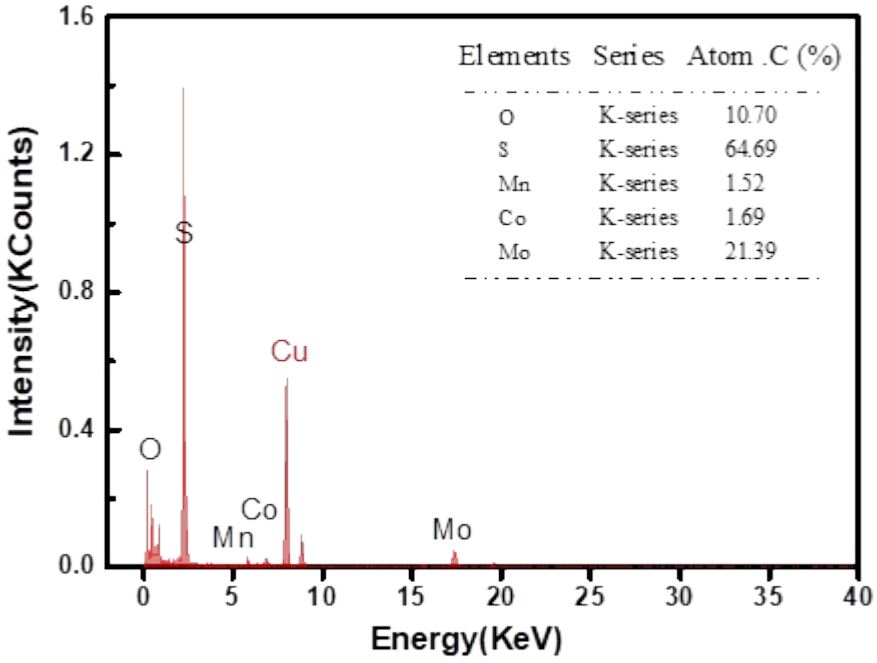

Fig. S6. EDS images of the Co_4S_3-MnS-MoS_2@CC (Note: The Cu peak at ~8 keV corresponds to the copper grid used during sample preparation, and is not part of the sample itself)

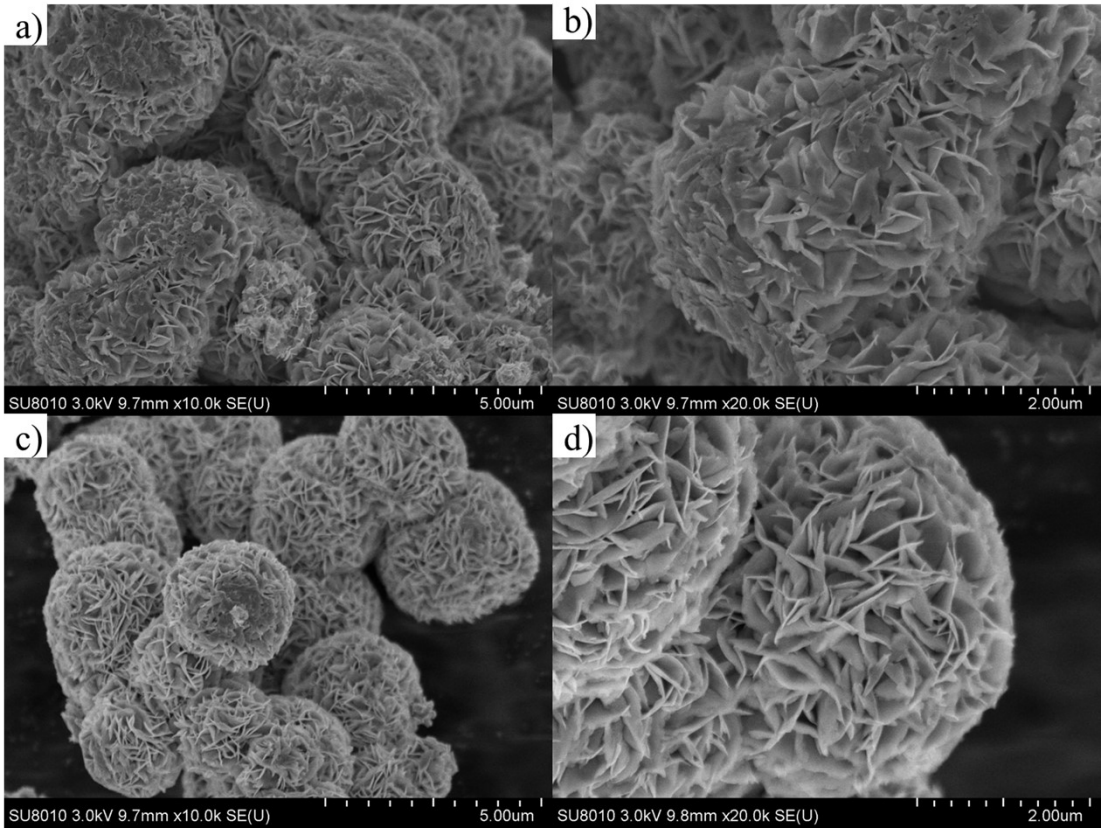

110 **Fig. S7. SEM images of the Co_4S_3-MnS-MoS_2@CC; a-b) before calcination**

111 **; c-d) after calcination**

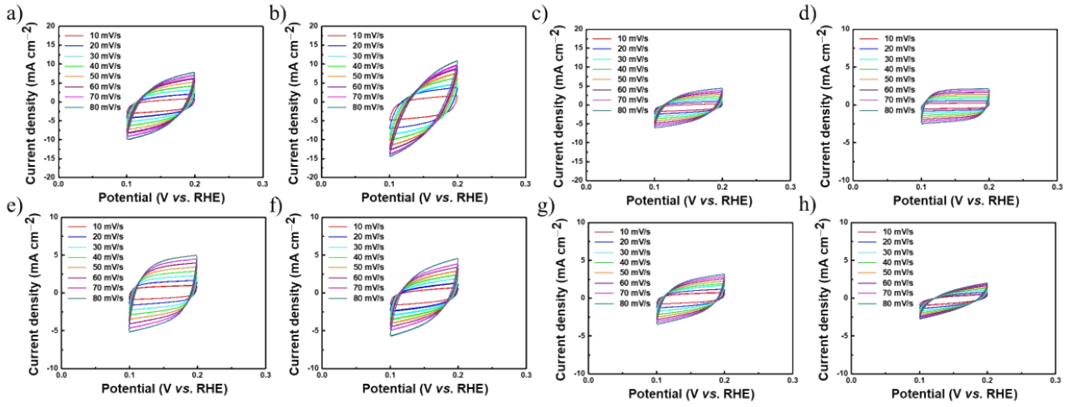

112

113 **Fig. S8. CV of Co_4S_3-MnS-MoS_2@CC, MnS-MoS_2@CC, Co_xS-MoS_2@CC**

114 **and MoS_2@CC tested at various scan rates from 10 to 80 mV/s. a-c) In 1 M KOH;**

115 **d-f) In 0.5 M H_2SO_4**

116

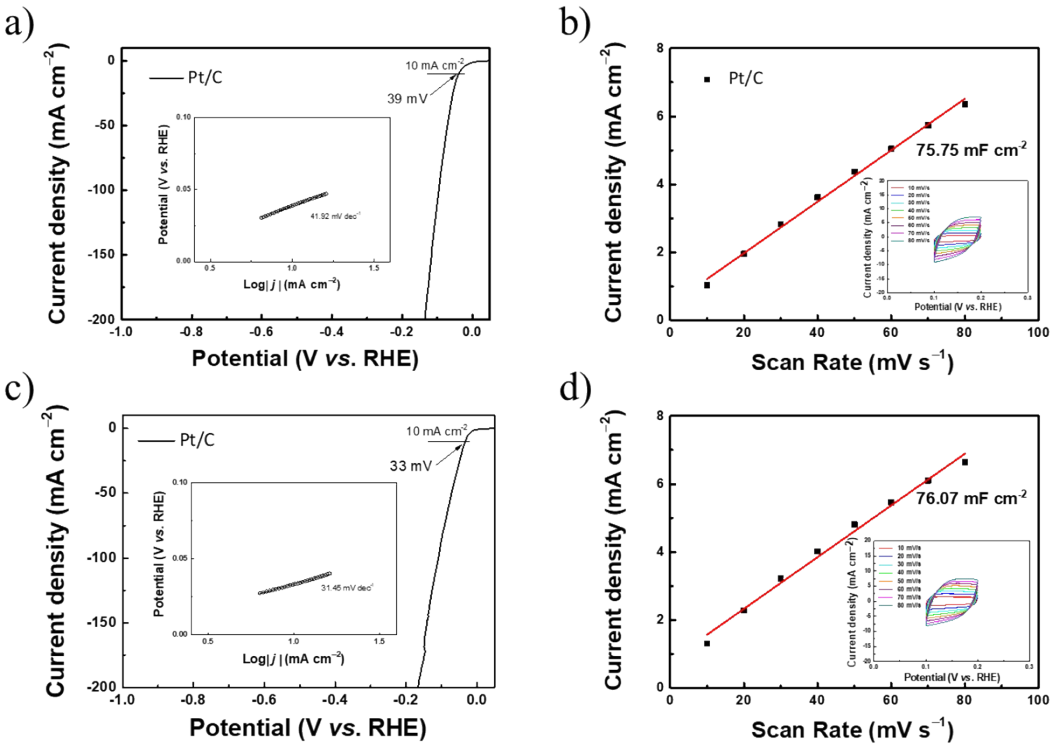

117 **Fig. S9. HER performance of the Pt/C@CC. a-b) In 1 M KOH; c-d) In 0.5**

118 **M H_2SO_4**

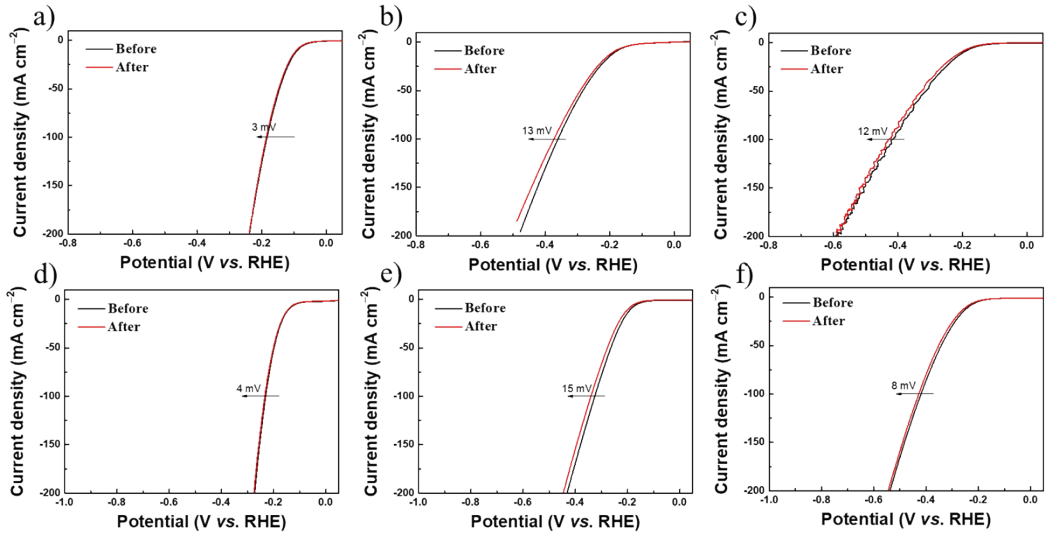

119

120 **Fig. S10. a-b) Polarization curves of Co_4S_3-MnS-MoS_2@CC, MnS-MoS_2@CC**

121 **and MoS_2@CC before and after 5000 CV cycles. a-c) In 1 M KOH; d-f) In 0.5 M**

122 **H_2SO_4**

123

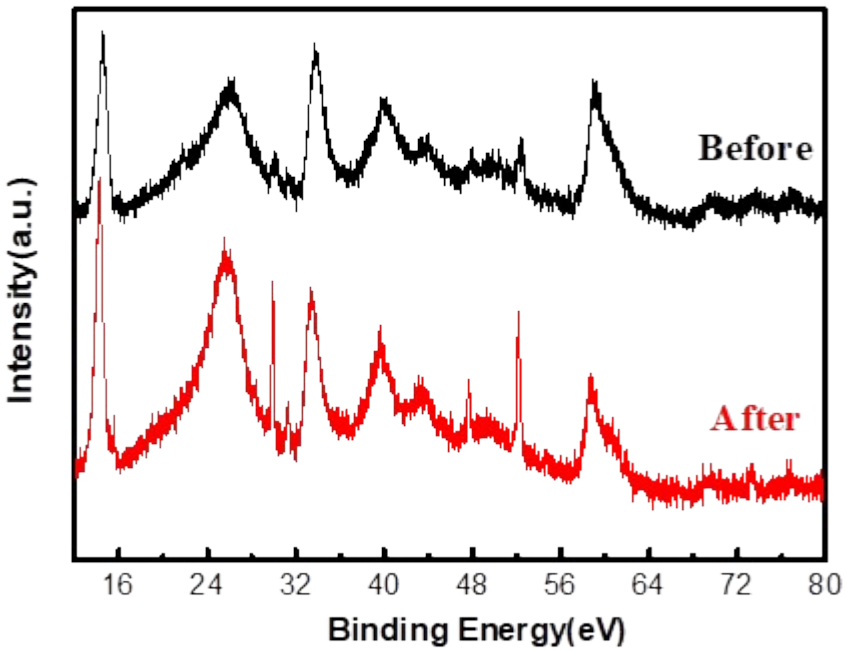

124 **Fig. S11. XRD patterns of Co_4S_3-MnS-MoS_2@CC**

125

126

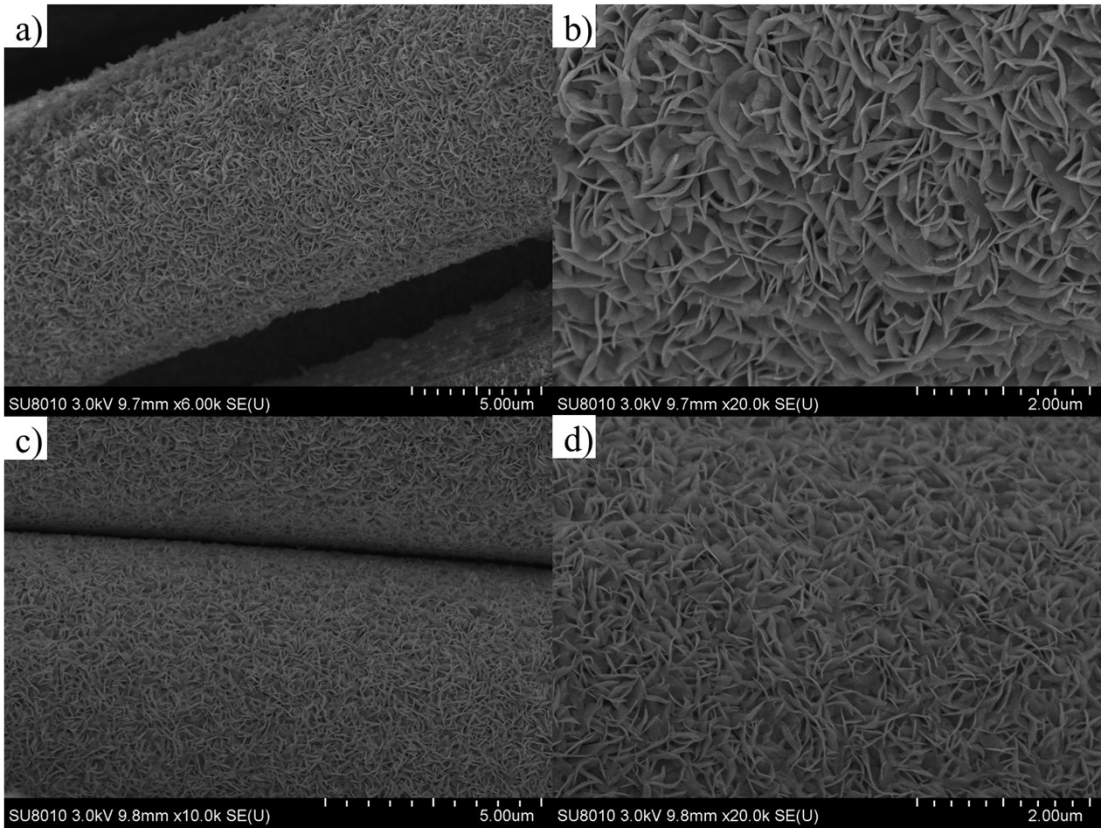

Fig. S12. SEM images of the Co_4S_3-MnS-MoS_2@CC. a-b) After i-t tests in 1 M KOH; c-d) After i-t tests in 0.5 M H_2SO_4

Catalyst	LSV/ η_{10}/mV	Ref.
Co_4S_3-MnS-MoS_2@CC	88	this work
Ni_4Mo	51	S.Energy Fuels.2024,8(8),1619-1625.[3]
CoS_2-MoS_2	251	J. Alloy.Compd.2023,948,169655.[4]
NC@MoS_2	145	J.Hydrogen Energy. 2024,56,570-581.[5]
NiO/MoS_2/$BiVO_4$	95	J.Hydrogen Energy. 2024,52,275-287.[6]
Ce-NiMoO4 /MoS2@rGO	153	ACS Applied Engineering Materials, 2024.[7]
MoS_2-Ni_3S_2-CNTs/NF	169	J.Hydrogen Energy.2024,91,196-203.[8]
TM SAs-MoS_2	80	A.Energy Materials.2024,14(35),2401716.[9]
1T-2H MoS_2	212	Chem Engineering J. 2023, 460,141858.[10]
$(NH_4)_2MoS_4$	248	Inorganic Chem.2023, 62(2),841-852.[11]
N-MoS_2/COF-C_4N	106	Catalysts.2023, 13(1),90.[12]
AC/MoS_2	136	J.Hydrogen Energy.2024, 55,1360-1370.[13]
Co-1T-MoS_2-bpe	118	A.Chemie 2023,135(48), e202313845.[14]
Co–MoS_2/Ni_3S_2/Ni	43	J.Hydrogen Energy.2024, 67,42-49.[15]

Table S1. Comparison of HER performance of Co_4S_3-MnS-MoS_2@CC catalyst with reported MoS_2-based catalysts in 1 M KOH

Reference:

[1] D. Zammel, I. Nagazi, A. Haddad, Synthesis and Characterization of a Novel Waugh-Type Polyoxometalate K1.5(NH4)4.5[MnMo9O32]·4.2H2O, Journal of Cluster Science 26(5) (2015) 1693-1706. https://doi.org/10.1007/s10876-015-0868-8.

[2] C. Wang, H. Zhan, X. Lu, R. Jing, H. Zhang, L. Yang, X. Li, F. Yue, D. Zhou, Q. Xia, A recyclable cobalt(iii)–ammonia complex catalyst for catalytic epoxidation of olefins with air as the oxidant, New Journal of Chemistry 45(4) (2021) 2147-2156. https://doi.org/10.1039/D0NJ05466F.

[3] D. Wei, S. Yanmei, Z. Wei, Y. Yifu, Z. Bin, Unveiling the In Situ Dissolution and Polymerization of Mo in Ni4Mo Alloy for Promoting the Hydrogen Evolution Reaction, Angewandte Chemie 133(13) (2021) 7127-7131. https://doi.org/10.1002/anie.202015723.

[4] P. Cao, X. Zhang, L. Wang, H. Fu, Alloying Ni4Mo for efficient alkaline hydrogen oxidation and hydrogen evolution reactions, Sustainable Energy & Fuels 8(8) (2024) 1619-1625. https://doi.org/10.1039/D4SE00179F.

[5] K. Chanda, P. Bairi, S. Maiti, A. Tripathi, R. Thapa, S. Ghosh, K. Panigrahi, D. Roy, R. Sarkar, K.K. Chattopadhyay, Crystallinity and interfacial Mo–N–C bond engineered MoS2 embedded graphitic nitrogen doped carbon hollow sphere for enhanced HER activity, International Journal of Hydrogen Energy 56 (2024) 570-581. https://doi.org/https://doi.org/10.1016/j.ijhydene.2023.12.159.

[6] K.K. Mandari, S. Pandey, M. Kang, Highly efficient ternary NiO/MoS2/BiVO4 heterostructure for electrocatalytic HER/OER applications, International Journal of Hydrogen Energy 52 (2024) 275-287. https://doi.org/https://doi.org/10.1016/j.ijhydene.2023.07.058.

[7] M. Ali, M. Wahid, K. Majid, Tailored Ce-Doped NiMoO4/MoS2@rGO Nanoarchitectures for Sustainable Electrochemical Water Splitting in Alkaline Medium, ACS Applied Engineering Materials (2024). https://doi.org/10.1021/acsaenm.4c00533.

[8] L. Li, X. Li, H. Li, Self-supported MoS2-Ni3S2-CNTs/NF electrodes with super-hydrophilic multistage micro-nanostructures for efficient bifunctional monolithic water splitting, International Journal of Hydrogen Energy 91 (2024) 196-203. https://doi.org/https://doi.org/10.1016/j.ijhydene.2024.10.041.

[9] MengLi, XuanWang, HanDu, WenrouDong, SongboYe, HengLiu, HuameiSun, KaiHuang, HaoLi, YawenTang, GengtaoFu, Oxophilic Tm-Sites in MoS2 Trigger Thermodynamic Spontaneous Water Dissociation for Enhanced Hydrogen Evolution, Advanced Energy Materials 14(35) (2024) 2401716-2401716. https://doi.org/10.1002/aenm.202401716.

[10] Z. Hong, W. Hong, B. Wang, Q. Cai, X. He, W. Liu, Stable 1T –2H MoS2 heterostructures for efficient electrocatalytic hydrogen evolution, Chemical Engineering Journal 460 (2023) 141858. https://doi.org/https://doi.org/10.1016/j.cej.2023.141858.

[11] S. Venkateshwaran, A. Ajith, V. Duraisamy, A. Krishnan, S.M. Senthil Kumar, Tailoring of 1T Phase-Domain MoS2 Active Sites with Bridging S22– /Apical S2– Phase-Selective Precursor Modulation for Enriched HER Kinetics, Inorganic Chemistry 62(2) (2023) 841-852. https://doi.org/10.1021/acs.inorgchem.2c03608.

[12] N. Zhang, Z. Yang, W. Liu, F. Zhang, H. Yan, Novel Bifunctional Nitrogen Doped MoS2/COF-C4N Vertical Heterostructures for Electrocatalytic HER and OER, Catalysts 13(1) (2023) 90. https://doi.org/10.3390/catal13010090.

[13] A.M. Homayounfard, M. Maleki, H. Ghanbari, M.H. Kahnamouei, B. Safaei, Growth of few-layer flower-like MoS2 on heteroatom-doped activated carbon as a hydrogen evolution reaction electrode, International Journal of Hydrogen Energy 55 (2024) 1360-1370. https://doi.org/https://doi.org/10.1016/j.ijhydene.2023.11.123.

[14] H. Liu, S. Zhang, Y. Chai, B. Dong, Ligand Modulation of Active Sites to Promote Cobalt-Doped 1T-MoS2 Electrocatalytic Hydrogen Evolution in Alkaline Media, Angewandte Chemie 135(48) (2023). https://doi.org/10.1002/anie.202313845.

[15] X. Tang, Y. Zhang, Y. Zhang, X. Liu, J. Cao, C. Zhang, Three-dimensional Co–MoS2/Ni3S2/Ni assembly with interfacial engineering and electronic modulation for efficient hydrogen evolution reaction, International Journal of Hydrogen Energy 67 (2024) 42-49. https://doi.org/https://doi.org/10.1016/j.ijhydene.2024.04.144.